

## Predictive Mathematical Modelling of the Total Number of COVID-19 Cases for The United States

Hafeez Muhammad Yakasai<sup>1\*</sup> and Mohd Yunus Abd Shukor<sup>2</sup>

<sup>1</sup>Department of Biochemistry, Faculty of Basic Medical Sciences, College of Health Science, Bayero University Kano PMB 3011, Nigeria.

<sup>2</sup>Department of Biochemistry, Faculty of Biotechnology and Biomolecular Sciences, Universiti Putra Malaysia, 43400 UPM Serdang, Selangor, Malaysia.

\*Corresponding author:

Dr. Hafeez Muhammad Yakasai,  
Department of Biochemistry, Faculty of Basic Medical Sciences,  
College of Health Science, Bayero University, Kano  
P. M. B 3011, Kano State Nigeria  
Tel: +2348034966925  
Email: [hmyakasai.bch@buk.edu.ng](mailto:hmyakasai.bch@buk.edu.ng)

### HISTORY

Received: 25<sup>th</sup> Feb 2020  
Received in revised form: 14<sup>th</sup> of March 2020  
Accepted: 18<sup>th</sup> of May 2020

### KEYWORDS

Total infection  
COVID-19  
pandemic  
MMF  
mathematical model

### ABSTRACT

The current global COVID-19 pandemic is causing a lot of deaths and economic losses worldwide. The modelling of future death and cases is a very important aspect of managing the severity of the pandemic. In this paper, we demonstrated potential use of various growth models like modified Gompertz, Von Bertalanffy, Baranyi-Roberts, modified Logistics, Morgan-Mercer-Flodin (MMF), modified Richards and Huang in modeling the epidemic trend of COVID-19 in the form of total number of infection cases of SARS-CoV-2 in the United States as at 20<sup>th</sup> July 2020. The Morgan-Mercer-Flodin (MMF) model showed best fitting to the data set with least RMSE and AICc and the highest adjusted  $R^2$  values. The values for Accuracy and Bias Factors were closest to 1.0. Despite this, further statistical diagnosis of the data showed nonnormality with the residuals failing the runs and homoscedasticity tests. Interestingly, this was addressed by remodeling the data from day 132 onwards using the MMF model, which results in improving the statistical diagnosis. The fitting coefficients obtained include maximum growth rate ( $\log \mu_m$ ) of 0.03 (95% CI 0.023 - 0.039), curve constant ( $\delta$ ) that affects the inflection point of 1.42 (95% CI 1.304 - 1.540), lower asymptote value ( $\beta$ ) of 6.454 (95% CI 6.451 - 6.456) and maximal total number of cases ( $y_{max}$ ) of 7,906,786 (95% CI 6,652,732 - 10,839,269). The MMF model predicted that by 20<sup>th</sup> of August 2020 the total number of cases in the United States will be 5,560,168 (95% CI of 5,295,337 - 5,838,243), while the figure will rise to 6,366,506 (95% CI of 5,791,751 - 6,998,298) by 20<sup>th</sup> of September 2020. The predictive potential of the utilized model makes it a powerful tool for epidemiologist monitoring the severity of SARS-CoV-2 (COVID-19) in the United States in the near future. Although, predictions from this model as with any other model, need to be taken with caution due to unpredictable nature of COVID-19 situation locally and globally.

### INTRODUCTION

The newly emerged corona virus, SARS-CoV-2, which appeared in Wuhan China, in the last quarter of 2019, has spread to all corners of the world inflicting acute and severe health and economic catastrophe in both developed and developing countries, bringing the world to a near-complete standstill for the first time in a century [1,2,3,4]. The virus belongs to the family of coronavirus (CoV), that have previously given rise to many zoonotic infections over the past centuries [4]. COVID-19 was declared global pandemic on 11<sup>th</sup> of March 2020 and is still ravaging the humanity with current death tolls exceeding half a

million individuals and higher than 10 million people are infected worldwide. In the United States alone, there are more than 3.9 million infected case and approximately 142,000 death cases as at 20<sup>th</sup> July 2020.

Microorganisms such as bacteria and viruses showed sigmoidal growth pattern (curve) on their substrate (nutrients) including human, starting with a lag period ( $\lambda$ ) just after  $t = 0$ , followed by logarithmic (exponential) and stationary phases and finally the organism enters the death phase. To describe microbial growth curve and obtain important fitting parameters like lag period ( $\lambda$ ), maximum specific growth rate ( $\mu_m$ ) and

asymptotic values ( $A$ ), various sigmoidal functions including Morgan-Mercer-Flodin (MMF), modified Gompertz, modified Richards, Von Bertalanffy, Baranyi-Roberts and modified Logistics are utilized.

Mathematical models including quantitative, theoretical and simulation could be used to predict COVID-19 pandemic cases in the United States. Models such as von Bertalanffy, modified Gompertz and logistics have shown good predictive ability in modelling the COVID-19 pandemic [5]. This work is aimed at assessing the robustness of various available models like Gompertz [6,7], Richards [7,8], Morgan-Mercer-Flodin (MMF) [9], Logistic [7,10], Buchanan three-phase [11], Baranyi-Roberts [12], Von Bertalanffy [13,14] and recently Huang model [15] in fitting and evaluating the total infection case of SARS-CoV-2 (epidemic trend of COVID-19) in the United States by 20<sup>th</sup> of July 2020.

**MATERIALS AND METHODS**

Data from Worldometer was used to acquire the total number of infected cases in the United States as at 20<sup>th</sup> of July 2020 [16]. The data set was converted to logarithmic values, while considering the data after the first 20 infection cases as the starting time.

**Statistical analysis**

The frequently used statistical discriminators like Root-Mean-Square Error (RMSE), adjusted coefficient of determination ( $R^2$ ) and corrected AICc (Akaike Information Criterion), were used to find the best fitting model. RMSE was calculated based on Eqn. (1) [17], the smaller the number of parameters the smaller RMSE value.  $n$  is the number of experimental data,  $p$  is the number of parameters, while  $Pd_i$  and  $Ob_i$  are predicted and experimental data, respectively.

$$RMSE = \sqrt{\frac{\sum_{i=1}^n (Pd_i - Ob_i)^2}{n - p}} \tag{Eqn. 1}$$

The adjusted  $R^2$  was used to determine the quality of nonlinear model, thus overcome the number of parameters in a model ignored by coefficient of determination,  $R^2$ . In equations Eqns. 2 and 3, RMS is the Residual Mean Square, while the total variance of  $y$ -variable is denoted by  $S_y^2$ .

$$Adjusted (R^2) = 1 - \frac{RMS}{S_y^2} \tag{Eqn. 2}$$

$$Adjusted (R^2) = 1 - \frac{(1 - R^2)(n - 1)}{(n - p - 1)} \tag{Eqn. 3}$$

The AIC, equilibrate between the goodness of fit of a model, and the complexity of that model and is based on information theory [18]. However, corrected Akaike information criterion (AICc) was used to handle data with a smaller number of values or having a high number of parameters [19]. The AICc is calculated as follows (Eqn. 4), where  $n$  indicate the quantity of data points and  $p$  signifies the quantity of parameters. Thus, a model with smallest AICc value is considered more likely correct [19].

$$AICc = 2p + n \ln \left( \frac{RSS}{n} \right) + 2(p+1) \frac{2(p+1)(p+2)}{n-p-2} \tag{Eqn. 4}$$

The Accuracy and Bias factors (AF and BF) were calculated according to Ross [20] suggestion as follows;

$$\text{Bias factor} = 10 \left( \frac{\sum_{i=1}^n \log \left( \frac{Pd_i / Ob_i}{n} \right)}{n} \right) \tag{Eqn. 5}$$

$$\text{Accuracy factor} = 10 \left( \frac{\sum_{i=1}^n \log \left( \frac{|Pd_i / Ob_i|}{n} \right)}{n} \right) \tag{Eqn. 6}$$

**Data fitting**

GraphPad Prism software (v 8.0) was used to conduct nonlinear regression to fit-in the SARS-CoV-2 infection cases using various growth curve models (Table 1).

**Table 1:** Models used in fitting the SARS-CoV-2 infection cases in the United States.

Model	p	Equation
Modified Logistic	3	$y = \frac{A}{1 + \exp \left[ \frac{4\mu_m}{A} (\lambda - t) + 2 \right]}$
Modified Gompertz	3	$y = A \exp \left\{ -\exp \left[ \frac{\mu_m e}{A} (\lambda - t) + 1 \right] \right\}$
Modified Richards	4	$y = A \left\{ 1 + v \exp(1+v) \exp \left[ \frac{\mu_m}{A} (1+v) \left( 1 + \frac{1}{v} \right) (\lambda - t) \right] \right\}^{\left( \frac{-1}{v} \right)}$
Morgan-Mercer-Flodin (MMF)	4	$y = y_{max} - \frac{(y_{max} - \beta)}{1 + (\mu_m t)^\delta}$
Baranyi-Roberts	4	$y = A + \mu_m x + \frac{1}{\mu_m} \ln \left( e^{-\mu_m x} + e^{-h_0} - e^{-\mu_m x - h_0} \right) - \ln \left[ 1 + \frac{\mu_m x - 1 - \ln \left( e^{-\mu_m x} + e^{-h_0} - e^{-\mu_m x - h_0} \right)}{e^{0 \max - A}} \right]$
Von Bertalanffy	3	$y = K \left[ 1 - \left( \frac{A}{K} \right)^3 \exp \left( -\mu_m x / 3K \right) \right]^3$
Huang	4	$y = A + y_{max} - \ln \left( e^A + \left( e^{y_{max} - e^A} \right) e^{-\mu_m B(x)} \right)$ $B(x) = x + \frac{1}{\alpha} \ln \frac{1 + e^{-\alpha(x-\lambda)}}{1 + e^{\alpha \lambda}}$
Buchanan Three-phase model	3	Y = A, IF X < LAG Y = A + K(X - λ), IF λ ≤ X ≤ X <sub>MAX</sub> Y = Y <sub>MAX</sub> , IF X ≥ X <sub>MAX</sub>

Note:  
 A= maximum no of cases lower asymptote;  
 y<sub>max</sub>= maximum no of cases upper asymptote;  
 μ<sub>m</sub>= maximum specific growth rate;  
 v= affects near which asymptote maximum no of cases occurs.  
 λ=lag time  
 e = exponent (2.718281828)  
 t = time after first case is reported  
 α, β, δ and k = curve fitting parameters  
 h<sub>0</sub> = a dimensionless parameter quantifying the initial physiological state of the reduction process.  
 The lag time (h<sup>-1</sup>) or (d<sup>-1</sup>) can be calculated as h<sub>0</sub> = μ<sub>m</sub>  
 When data at time zero is 0 (Day after 1<sup>st</sup> case log 1=0 for COVID-19) the MMF is reduced to a 3-parameter model

**RESULTS AND DISCUSSION**

Following the fitting exercise involving eight different models, it was revealed that all the tested models except for Buchanan-3-phase model show visually acceptable fitting (Figs 1 to 6). Morgan-Mercer-Flodin (MMF) was best performing model with least RMSE, AICc and highest adjusted  $R^2$  values. The model also has an excellent Accuracy and Bias factors with values closest to 1.0 (Table 2). The fitting coefficients for the Morgan-Mercer-Flodin (MMF) model are shown in Table 3.

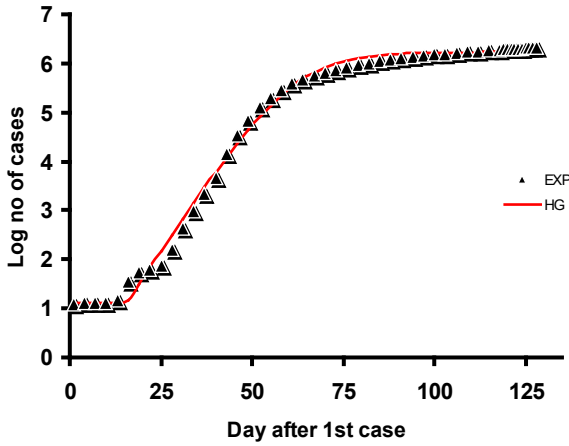


Fig. 1. Total number of SARS-CoV-2 infected cases in the United States as at 20<sup>th</sup> July 2020, as modelled using the Huang model.

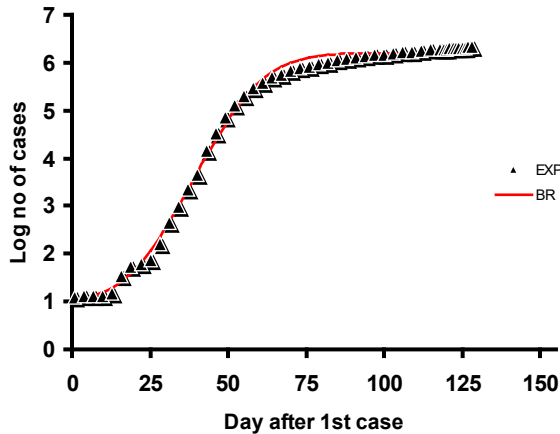


Fig. 2. Total number of SARS-CoV-2 infected cases in the United States as at 20<sup>th</sup> July 2020, as modelled using Baranyi-Roberts model.

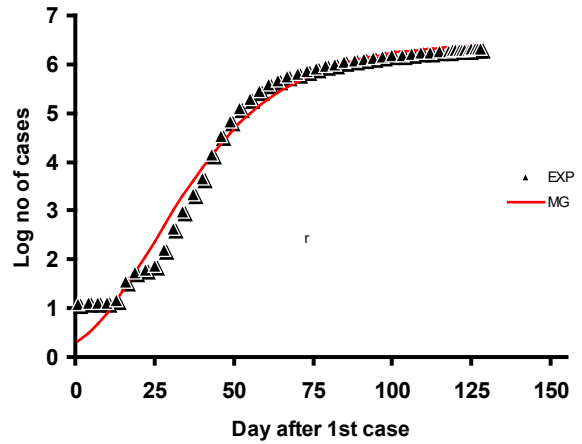


Fig. 3. Total number of SARS-CoV-2 infected cases in the United States as at 20<sup>th</sup> July 2020, as modelled using modified Gompertz model.

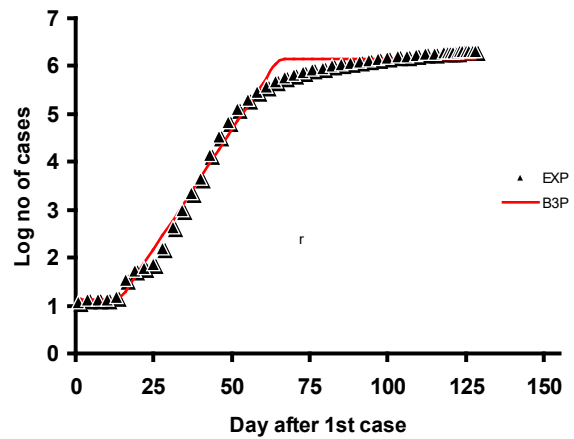


Fig. 4. Total number of SARS-CoV-2 infected cases in the United States as at 20<sup>th</sup> July 2020, as modelled using Buchanan-3-phase model.

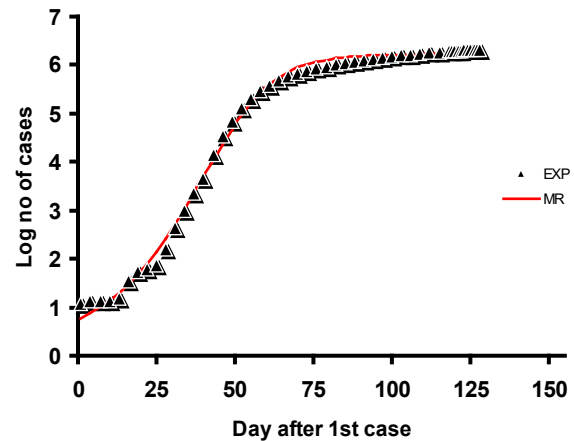


Fig. 5. Total number of SARS-CoV-2 infected cases in the United States as at 20<sup>th</sup> July 2020, as modelled using modified Richard model.

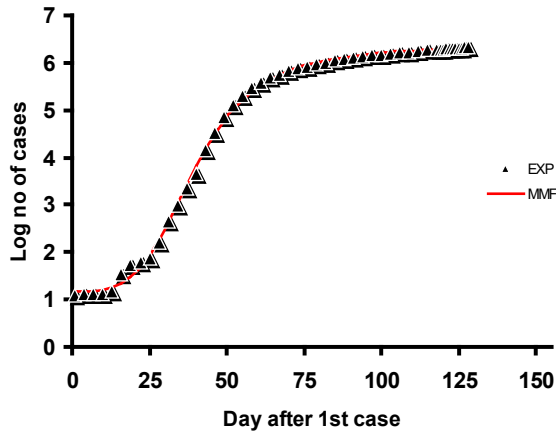


Fig. 6. Total number of SARS-CoV-2 infected cases in the United States as at 20<sup>th</sup> July 2020, as modelled using Morgan-Mercer-Flodin (MMF) model.

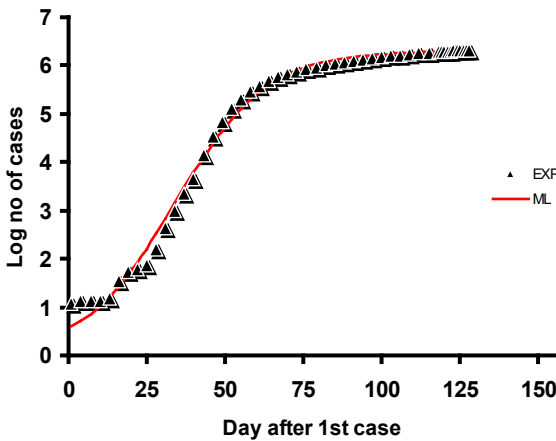


Fig. 7. Total number of SARS-CoV-2 infected cases in the United States as at 20<sup>th</sup> July 2020, as modelled using modified logistics model.

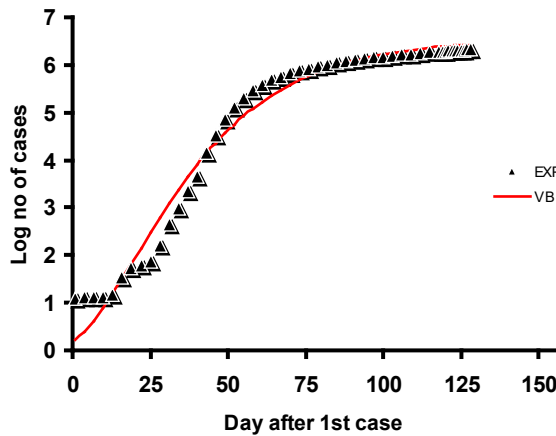


Fig. 8. Total number of SARS-CoV-2 infected cases in the United States as at 20<sup>th</sup> July 2020, as modelled using von Bertalanffy model.

Table 2. Statistical tests for various models utilized in modelling the total number of SARS-CoV-2 infected cases in the United States as at 15<sup>th</sup> July 2020.

Model	<i>p</i>	RMSE	<i>R</i> <sup>2</sup>	<i>adR</i> <sup>2</sup>	AF	BF	AICc
Huang	4	0.131	0.996	0.995	1.014	1.00	-187.91
Baranyi-Roberts	4	0.111	0.997	0.997	1.013	1.00	-204.19
modified Gompertz	3	0.244	0.985	0.984	1.021	1.00	-129.36
Buchanan-3-phase	3	0.178	0.992	0.991	1.021	1.00	-160.97
modified Richards	4	0.118	0.996	0.996	1.012	1.00	-198.22
MMF	4	0.073	0.999	0.998	1.006	1.00	-245.99
modified Logistics	3	0.151	0.994	0.994	1.012	1.00	-177.22
von Bertalanffy	3	0.291	0.979	0.977	1.027	1.00	-111.59

Note: *p* is number of parameters

Table 3. Coefficients as modelled using Morgan-Mercer-Flodin (MMF) model.

Parameters	Value	95% Confidence interval
$\mu_m$	0.060	0.057 to 0.063
$\delta$	1.553	1.425 to 1.688
$y_{max}$	4,305,266	3,706,807 to 5,093,309
$\beta$	2.550	2.414 to 2.677

Table 4. Predictions of COVID-19 pandemic for the United States based on the Morgan-Mercer-Flodin (MMF) model.

Prediction	Mean	95% Confidence interval
Maximum number of total infected cases by the end of COVID-19	4,305,266	3,706,807 to 5,093,309
Maximum number of total infected cases by 15 <sup>th</sup> August 2020	3,150,889	2,914,497 to 3,406,455
Maximum number of total infected cases by 15 <sup>th</sup> September 2020	3,399,583	3,108,520 to 3,717,899

The fitting coefficients obtained from Morgan-Mercer-Flodin (MMF) model were maximum growth rate ( $\log \mu_m$ ) of 0.03 (95% CI 0.030 - 0.036), curve constant ( $\delta$ ) that affects the inflection point of 1.100 (95% CI 1.029 - 1.171), lower asymptote value ( $\beta$ ) of 2.55 (95% CI 2.414 - 2.677) and maximal total number of cases ( $y_{max}$ ) of 4,305,266 (95% CI 3,706,807 - 5,093,309). This model predicted that the total number of infected cases in the United States by 20<sup>th</sup> August 2020 will be 384,258 (95% CI 368,567 - 400,618) and by 20<sup>th</sup> September 2020 will rise to 508,412 (95% CI 482,797 - 535,387). This prediction has to be used with caution since the model underpredicts the number of days for the current number of cases (4,028,529 cases as at 21<sup>st</sup> July 2020).

The major reason for this discrepancy appears likely to be due to data from June 25<sup>th</sup> 2020 onwards (roughly day 132 onwards), which seems not adequately modelled by the Morgan-Mercer-Flodin (MMF) model. A nonlinear trend was observed on visual inspection of the nonlogarithmic data (Fig. 9) from this point onwards. This unconformity to the MMF model is obvious when using statistical diagnostics for the curve where the residuals failed most of the normality and homoscedasticity tests (Table 5).

**Table 5.** Statistical diagnostic tests for the Morgan-Mercer-Flodin (MMF) model.

Tests	Diagnostic assessment
Normality of Residuals	
Anderson-Darling (A2*)	1.556
P value	0.0005
Passed normality test (alpha=0.05)?	No
P value summary	***
D'Agostino-Pearson omnibus (K2)	4.578
P value	0.1013
Passed normality test (alpha=0.05)?	Yes
P value summary	ns
Shapiro-Wilk (W)	0.9239
P value	0.0033
Passed normality test (alpha=0.05)?	No
P value summary	**
Kolmogorov-Smirnov (distance)	0.1523
P value	0.0054
Passed normality test (alpha=0.05)?	No
P value summary	**
Runs test	
Points above curve	23
Points below curve	27
Number of runs	5
P value (runs test)	<0.0001
Deviation from Model	Significant
Test for homoscedasticity	
Rs of predicted Y vs.  residual	0.2563
P value (one tailed)	0.0362
Passed (P > 0.05)?	No

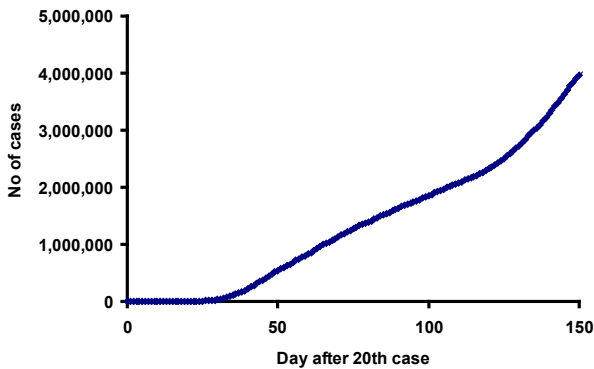


**Fig. 9.** Predictions of COVID-19 pandemic for the United States based on the Morgan-Mercer-Flodin (MMF) model after 132<sup>th</sup> infected case

The trend observed could be attributable to several underlying causes including an explosion in the infection rate due to lifestyle coupled with failure to strictly comply with lockdown or population rallying against lockdown measures. To better modelled the observed data, a discontinuous modelling was performed where total infected cases after day 132 onwards was remodelled using the Morgan-Mercer-Flodin (MMF) model. Results of the statistical analysis show improvement in all performing tests (Table 6).

**Table 6.** Statistical diagnostic tests for Morgan-Mercer-Flodin (MMF) model from day 132 onwards.

Normality of Residuals	
Anderson-Darling (A2*)	0.2663
P value	0.6496
Passed normality test (alpha=0.05)?	Yes
P value summary	ns
D'Agostino-Pearson omnibus (K2)	1.033
P value	0.5965
Passed normality test (alpha=0.05)?	Yes
P value summary	ns
Shapiro-Wilk (W)	0.9623
P value	0.6182
Passed normality test (alpha=0.05)?	Yes
P value summary	ns
Kolmogorov-Smirnov (distance)	0.1122
P value	>0.1000
Passed normality test (alpha=0.05)?	Yes
P value summary	ns
Runs test	
Points above curve	8
Points below curve	11
Number of runs	7
P value (runs test)	0.0882
Deviation from Model	Not Significant
Test for homoscedasticity	
Rs of predicted Y vs.  residual	0.1754
P value (one tailed)	0.2363
Passed (P > 0.05)?	Yes

The fitting parameters obtained from MMF remodelling include maximum growth rate ( $\log \mu_m$ ) of 0.03 (95% CI 0.023 - 0.039), curve constant ( $\delta$ ) that affects the inflection point of 1.42 (95% CI 1.304 - 1.540), lower asymptote value ( $\beta$ ) of 6.454 (95% CI 6.451 - 6.456) and maximal total number of infected cases ( $y_{max}$ ) of 7,906,786 (95% CI 6,652,732 - 10,839,269) (Table 7). The MMF predicted that total number of infected cases for United States by upcoming 20<sup>th</sup> August and 20<sup>th</sup> September 2020 will be 5,560,168 (95% CI 5,295,337 - 5,838,243) and 6,366,506 (95% CI 5,791,751 - 6,998,298), respectively (Table 8).

**Table 7.** Fitting coefficients for the Morgan-Mercer-Flodin (MMF) model after day 132 onwards data

Parameters	Value	95% Confidence interval
$\mu_m$	0.031	0.023 to 0.039
$\delta$	1.42	1.304 to 1.540
$y_{max}$	7,906,786	6,652,732 to 10,839,269
$\beta$	6.454	6.451 to 6.456

**Table 8.** Predictions of COVID-19 pandemic for the United States based on MMF model after day 132 onwards data.

Prediction	Mean	95% Confidence interval
Maximum number of total cases by the end of COVID-19	7,906,786	6,652,732 to 10,839,269
Maximum number of total cases by 15 <sup>th</sup> of August 2020	5,560,168	5,295,337 to 5,838,243
Maximum number of total cases by 15 <sup>th</sup> of September 2020	6,366,506	5,791,751 to 6,998,298

The Morgan-Mercer-Flodin (MMF) model was originally developed to describe a variety of nutrient-response relationships in higher organisms [9]. Presently, the MMF model has found usefulness in various modelling exercise involving animals such as horse, sheep, rabbit and as well microorganisms [21,22,23,24,25]. The model was also used to monitor yield of oil palm [26], ethanol [27] and in financial activities [28]. Perhaps, whether the prediction is correct or not will depend on a case by case basis and include effectiveness of lockdown, increase rate of infection due to mutation of the virus, to name a few. Certainly, the models will be revisited every few months to remodel the data so that a better prediction can be obtained.

## CONCLUSION

In conclusion, Morgan-Mercer-Flodin (MMF) model was the best fitting model in modelling the total number of SARS-CoV-2 infected cases in the United States as at 20<sup>th</sup> July 2020 based on statistical values for RMSE (root-mean-square error),  $R^2$  (adjusted coefficient of determination), AICc (corrected Akaike Information Criterion) BF (bias factor) and AF (accuracy factor) The MMF model predicted that by 20<sup>th</sup> of August 2020 the total number of cases in the United States will be 5,560,168 (95% CI of 5,295,337 - 5,838,243), while the figure will rise to 6,366,506 (95% CI of 5,791,751 - 6,998,298) by 20<sup>th</sup> of September 2020. This model permits the prediction of total number of cases, which will vary based on a number of factors. The predictive potential of the utilized model makes it a powerful tool for epidemiologist monitoring the severity of SARS-CoV-2 (COVID-19) in the United States in the near future.

## REFERENCES

- Segars J, Katler Q, McQueen DB, Kotlyar A, Glenn T, Knight Z, Feinberg EC, Taylor HS, Toner JP, Kawwass JF. Prior and novel coronaviruses, Coronavirus Disease 2019 (COVID-19), and human reproduction: what is known? *Fertility and Sterility* 2020;113: 1140–1149.
- Hageman JR. The Coronavirus Disease 2019 (COVID-19). *Pediatric Annals* 2020;49: e99–e100.
- Desforges M, Le Coupance A, Dubeau P, Bourgouin A, Lajoie L, Dubé M, Talbot PJ. Human Coronaviruses and Other Respiratory Viruses: Underestimated Opportunistic Pathogens of the Central Nervous System? *Viruses* 2020;12: 14.
- Gorbalenya AE, Baker SC, Baric RS, de Groot RJ, Drosten C, Gulyaeva AA, et al. Coronaviridae Study Group of the International Committee on Taxonomy of Viruses The species Severe acute respiratory syndrome-related coronavirus: classifying 2019-nCoV and naming it SARS-CoV-2. *Nature Microbiol.* 2020;5: 536–544.
- Jia L, Li K, Jiang Y, Guo X, Zhao T. Prediction and analysis of Coronavirus Disease 2019. 2020 *arXiv:200305447 [q-bio]*. <http://arxiv.org/abs/2003.05447>.
- Gompertz B. On the nature of the function expressiveness of the law of human mortality, and a new mode of determining the value of life contingencies. *Philos TransR Soc Lond.* 1825;115: 513–585.
- Zwietering MH, Jongenburger I, Rombouts FM, Van't Riet K. Modeling of the bacterial growth curve. *Appl Environ Microbiol.* 1990;56: 1875–1881.
- Richards FJ. A flexible growth function for empirical use. *J Exp Bot.* 1959;10: 290–300.
- Morgan PH, Mercer LP, Flodin NW (1975) General model for nutritional responses of higher organisms. *Proceedings of the Nat Acad Sci.* 1975;72: 4327–4331.
- Ricker WE. '11 Growth Rates and Models'. *Fish Physiol.* 1979; 8: 677-743.
- Buchanan RL. Predictive food microbiology. *Trends Food Sci Tech.* 1993;4: 6–11.
- Baranyi J (1995) Mathematics of predictive food microbiology. *Intl J Food Microbiol.* 1995;26: 199–218. doi:10.1016/0168-1605(94)00121-L.
- López S, Prieto M, Dijkstra J, Dhanoa MS, France J. Statistical evaluation of mathematical models for microbial growth. *Intl J Food Microbiol.* 2004;96: 289–300. doi: 10.1016/j.ijfoodmicro-2004.03.026.
- Babák L, Šupinová P, Burdychová R. Growth models of *Thermus aquaticus* and *Thermus scotoductus*. *Acta Universitatis Agriculturae et Silviculturae Mendelianae Brunensis.* 2012;60: 19–26. doi:10.11118/actaun201260050019.
- Huang L. Optimization of a new mathematical model for bacterial growth. *Food Contr.* 2013;32: 283–288. doi:10.1016/j.foodcont-2012.11.019.
- Worldometer. COVID-19 Coronavirus Pandemic. 2020 <https://www.worldometers.info/coronavirus/#countries>.
- Motulsky HJ, Ransnas LA. Fitting curves to data using nonlinear regression: a practical and nonmathematical review. *FASEB J.* 1987;1: 365–374.
- Akaike H. Factor analysis and AIC. *Psychometrika* 1987;52: 317–332. doi:10.1007/BF02294359.
- Burnham KP, Anderson DR. 'Model Selection and Multimodel Inference: A Practical Information-Theoretic Approach.' (Springer Science & Business Media). 2002
- Ross T, McMeekin TA. Predictive microbiology. *International J Food Microbiol.* 1994;23: 241–264. doi:10.1016/0168-1605(94)90155-4.
- Santos SA, Souza G da S e, Oliveira MR de, Sereno JR. Uso de modelos não-lineares para o ajuste de curvas de crescimento de cavalos pantaneiros. *Pesquisa Agropecuária Brasileira* 1999;34: 1133–1138.
- Topal M, Bolukbasi ŞC. Comparison of nonlinear growth curve models in broiler chickens. *J Appl Animal Res.* 2008;34: 149–152. doi:10.1080/09712119.2008.9706960.
- Tariq M, Iqbal F, Eyduran E, Bajwa M, Huma Z, Waheed A. Comparison of non-linear functions to describe the growth in Mengali sheep breed of Balochistan. *Pakistan J Zool.* 2013;45: 661–665.
- Augustine A, Imelda J, Paulraj R, David NS. Growth kinetic profiles of *Aspergillus niger* S14 a mangrove isolate and *Aspergillus oryzae* NCIM 1212 in solid state fermentation. *Indian J Fisheries.* 2015;62: 100–106.
- Kemper CM. Growth and development of the brush-tailed rabbit-rat (*Conilurus penicillatus*), a threatened tree-rat from northern Australia. *Australian Mammal.* 2020, doi:10.1071/AM19027.
- Khamis A, Ismail Z, Haron K, Mohammed AT. Nonlinear Growth Models for Modeling Oil Palm Yield Growth. *J Math Stat.* 2005; 1: 225–233. doi:10.3844/jmssp.2005.225.233.
- Germec M, Turhan I. Ethanol production from acid-pretreated and detoxified tea processing waste and its modeling. *Fuel* 2018;231: 101–109. doi:10.1016/j.fuel.2018.05.070.
- Wijeratne AW, Karunaratne JA. Morgan-Mercer-Flodin model for long term trend analysis of currency exchange rates of some selected countries. *Intl J Bus Excel.* 2013;7: 76–87. doi:10.1504/IJBEX.2014.057859.